Hydrophobic and hydrophilic interactions in aqueous mixtures of alcohols at a hydrophobic surface

Deepti Ballal and Walter G. Chapman

Citation: J. Chem. Phys. **139**, 114706 (2013); doi: 10.1063/1.4821604
View online: http://dx.doi.org/10.1063/1.4821604
View Table of Contents: http://jcp.aip.org/resource/1/JCPSA6/v139/i11
Published by the AIP Publishing LLC.

Hydrophobic and hydrophilic interactions in aqueous mixtures of alcohols at a hydrophobic surface

Deepti Ballal and Walter G. Chapman[a)]
Department of Chemical and Biomolecular Engineering, Rice University, 6100 S. Main, Houston, Texas 77005, USA

(Received 16 June 2013; accepted 4 September 2013; published online 20 September 2013)

Aqueous solutions of alcohols are interesting because of their anomalous behavior that is believed to be due to the molecular structuring of water and alcohol around each other in solution. The interfacial structuring and properties are significant for application in alcohol purification processes and biomolecular structure. Here we study aqueous mixtures of short alcohols (methanol, ethanol, 1-propanol, and 2-propanol) at a hydrophobic surface using interfacial statistical associating fluid theory which is a perturbation density functional theory. The addition of a small amount of alcohol decreases the interfacial tension of water drastically. This trend in interfacial tension can be explained by the structure of water and alcohol next to the surface. The hydrophobic group of an added alcohol preferentially goes to the surface preserving the structure of water in the bulk. For a given bulk alcohol concentration, water mixed with the different alcohols has different interfacial tensions with propanol having a lower interfacial tension than methanol and ethanol. 2-propanol is not as effective in decreasing the interfacial tension as 1-propanol because it partitions poorly to the surface due to its larger excluded volume. But for a given surface alcohol mole fraction, all the alcohol mixtures give similar values for interfacial tension. For separation of alcohol from water, methods that take advantage of the high surface mole fraction of alcohol have advantages compared to separation using the vapor in equilibrium with a water-alcohol liquid. © *2013 AIP Publishing LLC*. [http://dx.doi.org/10.1063/1.4821604]

I. INTRODUCTION

Aqueous solutions of alcohols are of interest because of their use as industrial solvents for separation processes and in fuel cells. They are interesting also because of the many anomalous properties they show such as a maximum in heat capacity and a minimum in partial molar volume.[1–4] Alcohols are also the simplest form of amphiphilic molecules having both hydrophobic and hydrophilic segments. Solvation of polar and non-polar segments in water is of importance in biomolecular systems. A good understanding of water-alcohol systems can help in the better understanding of aqueous solutions of more complex amphiphilic biomolecules which are difficult to study.

Thermodynamics and structure of water-alcohol mixtures are quite different in the water-rich and alcohol-rich region.[5,6] It is believed that the anomalous properties of water-alcohol mixtures arise from the structuring of water and alcohol molecules around each other in solution. The molecular structure of water and alcohol in solution is not completely understood; both water and alcohol form complex hydrogen bonded networks but the presence of hydrophobic alkyl groups in alcohols complicate the structuring in the solution. It is known that the mixing of water and alcohol is dominated by excess entropy more than excess enthalpy. It was earlier thought that the structure of water is enhanced around the hydrophobic segment of the alcohol causing the negative excess entropy of the system.[3] But recent scattering experiments have shown that there is no enhancement in the structure around the hydrophobic segments of the alcohol.[7–10] The hydrophobic segments cluster together and the anomalous properties of water-alcohol mixtures arise from the incomplete mixing of water and alcohol which leaves remnant hydrogen bonded networks of water leading to a negative excess entropy.[11] Molecular simulations support the idea that polar interactions between water and hydrophilic groups in alcohol are as important as hydrophobic interactions in water-alcohol systems.[12,13] A recent experimental study also showed a temperature dependence of hydrophobic hydration in alcohol water mixtures with enhanced structure of water around hydrophobic groups of alcohol at low temperature but a disordered structure at higher temperatures.[14]

Considerable effort has gone into studying aqueous alcohol mixtures in the bulk, but much less has been done for inhomogeneous systems. Understanding the thermodynamics and microstructure of aqueous alcohol under the influence of external factors is important for many applications like in separation processes. Separation of organic compounds and water is traditionally done through distillation or recrystallization techniques which require a lot of energy. Separation at an interface where there is a preferential concentration of one of the components at the interface is an alternative. Traditionally, the preparation of Japanese Sake has included passing air above a vapor-liquid interface and collecting the ethanol rich vapor phase to separate ethanol from water. Recently ultrasonic atomization has been used to separate ethanol from water by forming a mist, which is concentrated in ethanol, from

a)Author to whom correspondence should be addressed. Electronic mail: wgchap@rice.edu. Tel.: (1) 713 348 4900. Fax: (1) 713 348 5478.

a vapor-liquid interface.[15] Some of the other methods include using a membrane, like polydimethylsiloxane (PDMS), that is selectively permeable to one component much more than the other or the preferential adsorption of alcohols on surfaces (such as hydrophobic zeolites).[16] These different separation techniques can be optimized by understanding the structure of water and alcohol at the interface.[17]

Water-alcohol mixtures play an important role in biological systems as well. The melting temperature of t-RNA in an aqueous alcohol solution goes through a minima with increasing alcohol concentration.[18] The minimum occurs at a much lower mole fraction of 1-propanol than methanol showing the importance of competing hydrophobic and hydrophilic interactions in alcohol. This competition is important in protein structuring as well. Proteins fold perfectly into their three-dimensional native state in water, but are denatured when put in an organic solution like ethanol. It is known that the hydrophobic effect plays an important role in stabilizing the native structure of proteins in water.[19] Due to the presence of non-polar groups in alcohol, interactions of the amino acids in proteins are different in water and in alcohol. In fact, water-ethanol mixtures have been used to establish the hydrophobicity of amino acids.[20] Addition of glycerol, which has multiple hydroxyl groups, to water actually stabilizes the native structure of proteins further emphasizing the role of opposing hydrophobic and hydrophilic interactions.[21] An understanding of the structure of water and alcohol around hydrophobic surfaces would be helpful in better understanding the stabilization of the native structure of proteins.

Despite the importance of aqueous alcohol mixtures at solid hydrophobic surfaces very little work has been done there. Most inhomogeneous studies of aqueous mixtures of alcohols tend to concentrate on liquid-vapor interfaces.[22,23] Some studies have looked at the structure of aqueous solutions of amphiphilic molecules like alcohols next to hydrophilic surfaces and the effect of this structuring on the properties of the system.[24,25] But structural studies at a hydrophobic surface has been mainly for pure water.[26] Water-alcohol mixtures at a hydrophobic surface have only been studied for contact angle or structure of droplets.[27–29] Interaction between small hydrophobic molecules (like methane) in a mixture of water and ethanol was studied.[30] These studies show that ethanol at low concentration stabilizes the structure of water around the hydrophobic methane and the strength of hydrophobic interaction decreases with increasing alcohol concentration. There have not been any studies that have carefully studied the molecular structure of water-alcohol solution at a hydrophobic surface which is essential to understanding the governing physics of the system.

Recently Density Functional Theory (DFT) has emerged as a powerful theoretical tool to study the microstructure and thermodynamics of different inhomogeneous systems. An advantage of using DFT is that it is much faster than simulation and studies on trace components can be easily done. Chapman[31] was the first to recognize that Wertheim's first order thermodynamic perturbation theory (TPT1)[32] can be written in an inhomogeneous form in a DFT framework. Kierlik and Rosinberg[33,34] were the first to develop a perturbation DFT for polyatomic molecules.[32] Segura *et al.*[35] developed two DFTs for hydrogen bonding molecules using TPT1 as a basis. One of these was further developed by Yu and Wu for hydrogen bonding molecules and later polyatomic molecules.[36,37] Tripathi and Chapman[38] later proposed a polyatomic DFT now known as the inhomogeneous Statistical Associating Fluid Theory (iSAFT)[39] which was further modified by Jain *et al.*[39] to include hetronuclear polyatomic molecules. In the bulk limit, iSAFT goes to the well known SAFT equation of state.[40] The theory has been successfully applied to a wide variety of systems such as alkanes,[41] lipid bilayers,[39] and block copolymers.[42,43] Recently Bymaster and Chapman[44,45] extended the theory to hydrogen bonding chains. We follow their approach to calculate the free energy and equilibrium structure of the alcohol-water mixture.

In this work we study the microstructure and thermodynamics of aqueous mixtures of a series of short alcohols (methanol, ethanol, 1-propanol, and 2-propanol) next to a hydrophobic surface. The theory has been used previously to model pure water at hydrophobic surfaces and was found to predict the structure and properties of water around hydrophobic solutes well.[46] Mixtures of water with different polar and nonpolar molecules have been modeled in both the bulk and at an interface using a SAFT based approach.[47–50] Section II describes the model used for the alcohol and water and the theory used to obtain the structure and thermodynamic properties. In Sec. III we present the results for structure of water and alcohol next to the surface and how the hydrogen bonding network changes with the addition of alcohol. We also discuss how the structuring affects interfacial tension for the different alcohols.

II. THEORY

A. Model

Most simple liquids interact via strong repulsive forces and weak attractive forces. But an important part of the interaction in water and hydrophilic segments (like in alcohol) is the strong, directional hydrogen bonds they form which are important in determining its structure. Here water is modeled as a single sphere with four hydrogen bonding sites whereas alcohol is modeled as a chain of m tangentially bonded spherical segments with two hydrogen bonding sites on one segment.

The effective pair potential u(**12**) between a pair of unbonded segments 1 and 2 can be written as

$$u(\mathbf{12}) = u^{HS}(\mathbf{12}) + u^{att}(\mathbf{12}) + u^{assoc}(\mathbf{12}), \tag{1}$$

where $u^{HS}(\mathbf{12})$ is the hard sphere potential to account for the short-ranged repulsive force (excluded volume effects)

$$u^{hs}(\boldsymbol{r}_{\mathbf{12}}) = \begin{cases} \infty, \boldsymbol{r}_{\mathbf{12}} < \sigma \\ 0, \boldsymbol{r}_{\mathbf{12}} \geq \sigma, \end{cases} \tag{2}$$

where $\mathbf{r_{12}}$ is the distance between segments 1 and 2, and σ is the average diameter of the two segments. The long range attraction is approximated by a cut-and-shifted

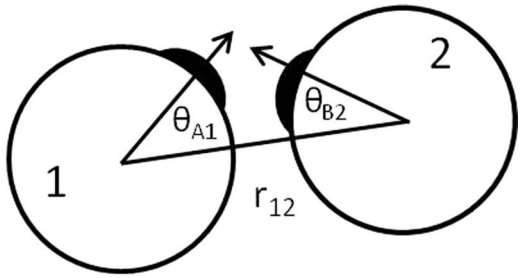

FIG. 1. Potential model for association (hydrogen bonding).

Weeks-Chandler-Anderson[51] attraction given by

$$u^{att}(\boldsymbol{r_{12}}) = \begin{cases} -\varepsilon^{LJ} - u^{LJ}(r_{cut}), & \sigma < \boldsymbol{r_{12}} < r_{min} \\ u^{LJ}(\boldsymbol{r_{12}}) - u^{LJ}(r_{cut}), & r_{min} < \boldsymbol{r_{12}} < r_{cut} \\ 0, & \boldsymbol{r_{12}} < r_{cut}, \end{cases} \tag{3}$$

where the minimum r_{min} is located at $2^{1/6}\sigma$ and the cutoff r_{cut} at 3σ; ε^{LJ} is the attraction energy and u^{LJ} is the Lennard-Jones (LJ) potential:

$$u^{LJ}(\boldsymbol{r_{12}}) = 4\varepsilon^{LJ}\left[\left(\frac{\sigma}{\boldsymbol{r_{12}}}\right)^{12} - \left(\frac{\sigma}{\boldsymbol{r_{12}}}\right)^{6}\right]. \tag{4}$$

Hydrogen bonds are characterized by short range directional interactions. We model hydrogen bonding as conical association sites present near the surface of the hard sphere.[52,53] Hydrogen bonding is modeled with a square well potential when two sites on two different molecules are within a certain distance of each other and are oriented in the right direction to imitate the short ranged directional hydrogen bonds (Figure 1). Hydrogen bonding potential for two sites A and B on molecules 1 and 2, respectively, is given by

$$u^{assoc}_{AB}(\boldsymbol{r_{12}}, \omega_1, \omega_2) = \begin{cases} -\varepsilon^{AB}, & \boldsymbol{r_{12}} < r_C; \theta_{A1} < \theta_C; \theta_{B2} < \theta_C \\ 0, & \text{Otherwise}, \end{cases} \tag{5}$$

where $\boldsymbol{r_{12}}$ is the distance between centers of the segments containing association sites on the two molecules. r_c ($=1.05\sigma$) is the cutoff distance and θ_C ($=27^\circ$) is the cutoff angle. There are two types of sites (O and H) for oxygen and hydrogen with only unlike sites being able to bond, i.e., $\varepsilon_{OO} = 0$, $\varepsilon_{HH} = 0$, and $\varepsilon_{OH} \neq 0$. Water is modeled as having four association sites—two O and two H. Alcohol is a chain of tangentially bonded hydrophobic and hydrophilic segments with the hydrophilic segments having two association sites—one O and one H.

Cross parameters for alcohol-water LJ interaction are given by

$$\varepsilon_{AW} = \sqrt{\varepsilon_A \varepsilon_W}\,(1 - k_{AW}) \quad ; \quad \sigma_{AW} = \tfrac{\sigma_A + \sigma_W}{2}, \tag{6}$$

where ε_A and ε_W are the alcohol and water energies, respectively; σ_A and σ_W are the alcohol and water diameters, respectively. k_{AW} is the binary interaction parameter for water-alcohol. For hydrogen bonding, the cross energy uses an arithmetic mean but a geometric mean is used for the hydrogen bond volume.

B. iSAFT density functional theory

Once we have an intermolecular potential model, we need a paradigm to calculate the inhomogeneous structure of the fluid. A density functional theory based in a grand canonical ensemble is used. The grand potential of the system (Ω), which is a functional of the density, can be related to the intrinsic Helmholtz free energy (A) using the Legendre transform

$$\Omega\left[\rho(\boldsymbol{r})\right] = A\left[\rho(\boldsymbol{r})\right] - \int d\boldsymbol{r_1} \sum_{i=1}^{N} \rho_i(\boldsymbol{r_1})\left(\mu_i^{bulk} - V_{ext}(\boldsymbol{r_1})\right). \tag{7}$$

The summation is over all segment types N in the system. $\rho_i(\boldsymbol{r_1})$ is the number density of segments of type i at position $\boldsymbol{r_1}$, μ_i^{bulk} is the bulk chemical potential of a segment of type i, and $V_{ext}(\boldsymbol{r_1})$ is the external potential at position $\boldsymbol{r_1}$. The external potential here is the hydrophobic surface modeled as a smooth hard wall

$$V_{ext}(r) = \begin{cases} 0, & r < (\sigma/2) \\ \infty, & r \geq (\sigma/2) \end{cases}, \tag{8}$$

where σ is the segment diameter. It is assumed that the liquid is homogenous in the directions along the surface and the inhomogeneity is only in the direction perpendicular to the surface. The equilibrium structure of the fluid produces a minimum in the grand potential:

$$\left.\frac{\delta\Omega[\rho(\boldsymbol{r})]}{\delta\rho(\boldsymbol{r})}\right|_{equilibrium} = 0 \Rightarrow \frac{\delta \mathrm{A}[\rho(\boldsymbol{r})]}{\delta\rho(\boldsymbol{r})} - (\mu - V_{ext}(\boldsymbol{r})) = 0. \tag{9}$$

The expression on the right can be solved for the equilibrium density profile if we have an expression for the intrinsic Helmholtz free energy as a functional of the density. Based on the potential model, the Helmholtz free energy has the following contributions:

$$A\left[\rho(\boldsymbol{r})\right] = A^{id}\left[\rho(\boldsymbol{r})\right] + A^{ex,hs}\left[\rho(\boldsymbol{r})\right] + A^{ex,att}\left[\rho(\boldsymbol{r})\right] + A^{ex,assoc}\left[\rho(\boldsymbol{r})\right] + A^{ex,chain}\left[\rho(\boldsymbol{r})\right], \tag{10}$$

where $A^{id}, A^{ex,hs}, A^{ex,att}, A^{ex,assoc}$, and $A^{ex,chain}$ are the ideal, hard sphere, long range attraction, association (hydrogen bonding), and chain contribution to the free energy. The chain term is relevant only for the alcohols. The ideal free energy is known exactly from statistical mechanics

$$\beta A^{id}\left[\rho(\boldsymbol{r})\right] = \int d\boldsymbol{r_1} \sum_{i=1}^{N} \rho_i(\boldsymbol{r_1})\left[\ln(\rho_i(\boldsymbol{r_1})) - 1\right]. \tag{11}$$

The temperature dependent de Broglie wavelength has been neglected here as it does not affect the structure of the fluid. Rosenfeld's Fundamental Measure Theory is used for the hard sphere contribution to the free energy[54]

$$\beta A^{ex,hs}\left[\rho(\boldsymbol{r})\right] = \int d\boldsymbol{r_1} \Phi^{ex,hs}\left[n_i(\boldsymbol{r_1})\right], \tag{12}$$

where $\Phi^{ex,hs}$ is the free energy density due to volume exclusion which is a function of the five fundamental measures ($n_i(\boldsymbol{r})$). The definition of the fundamental measures can be found in the paper by Rosenfeld. The free energy density is

given by

$$\Phi^{ex,hs}[n_i(\boldsymbol{r})] = -n_0 \ln(1-n_3) + \frac{n_1 n_2 - \boldsymbol{n}_{V1}\cdot\boldsymbol{n}_{V2}}{(1-n_3)} + \frac{{n_2}^3 - 3n_2 \boldsymbol{n}_{V2}\cdot\boldsymbol{n}_{V2}}{24\pi(1-n_3)^2}. \quad (13)$$

Long range attraction is approximated using a mean field theory

$$\beta A^{ex,att}[\rho(\boldsymbol{r})] = \iint d\boldsymbol{r_1} d\boldsymbol{r_2} \sum_{i=1}^{N}\sum_{j=1}^{N} \beta u_{ij}^{att}(|\boldsymbol{r_2}-\boldsymbol{r_1}|)\,\rho_i(\boldsymbol{r_1})\,\rho_j(\boldsymbol{r_2}), \quad (14)$$

where $\rho_i(\boldsymbol{r_1})$ and $\rho_j(\boldsymbol{r_2})$ are the density of segment types i and j at positions $\boldsymbol{r_1}$ and $\boldsymbol{r_2}$, respectively. For association free energy we use Wertheim's thermodynamic perturbation theory,[32] the inhomogeneous form of which was derived by Segura *et al.*[31,35]

$$\beta A^{ex,assoc}[\rho_i(\boldsymbol{r})] = \int d\boldsymbol{r_1} \sum_{i=1}^{N} \rho_i(\boldsymbol{r_1}) \sum_{A\in\Gamma^i}\left[\ln\chi_A^i(\boldsymbol{r_1}) - \frac{\chi_A^i(\boldsymbol{r_1})}{2} + \frac{1}{2}\right], \quad (15)$$

where $\chi_A^i(\boldsymbol{r_1})$ is the fraction of molecules of type i not bonded at site A at position $\boldsymbol{r_1}$. It can be obtained from a mass action equation

$$\chi_A^i(\boldsymbol{r_1}) = \frac{1}{1+\int d\boldsymbol{r_2}\sum_{k=1}^{N}\rho_k(\boldsymbol{r_2})\sum_{B\in\Gamma^k}\chi_B^k(\boldsymbol{r_2})\Delta_{AB}^{ik}(\boldsymbol{r_1},\boldsymbol{r_2})}. \quad (16)$$

The first sum in the denominator of the term on the right is over all the molecules k and the second summation is over all association sites B on molecule k. The condition for bonding is given by $\Delta_{AB}^{ik}(\boldsymbol{r_1},\boldsymbol{r_2}) = 4\pi\kappa\left[\exp\left(\beta\varepsilon_{Ai,Bk}^{assoc}\right)-1\right] y^{ik}(\boldsymbol{r_1},\boldsymbol{r_2})$. Here $\kappa = 0.25\,(1-\cos\theta_c)^2\,\sigma^2(r_c-\sigma)$ is the geometric constraint on the sites to be oriented in the right direction and be at the right distance from each other, $\varepsilon_{Ai,Bk}^{assoc}$ is the association energy between sites A and B on molecules i and k, respectively; and $y^{ik}(\boldsymbol{r_1},\boldsymbol{r_2})$ is the cavity correlation function for the inhomogeneous reference fluid. It is assumed that a site can bond only once; this assumption has worked well in the past for water and alcohol.[55,56] It is calculated as the geometric mean of the value at $\boldsymbol{r_1}$ and $\boldsymbol{r_2}$

$$y^{ik}(\boldsymbol{r_1},\boldsymbol{r_2}) = \left[y^{ik}\left(\overline{\rho_j}(\boldsymbol{r_1})\right)\times y^{ik}\left(\overline{\rho_j}(\boldsymbol{r_2})\right)\right]^{1/2}. \quad (17)$$

Here $\bar{\rho}_j(\boldsymbol{r_1})$ is the weighted density of segment j at position $\boldsymbol{r_1}$

$$\bar{\rho}_j(\boldsymbol{r_1}) = \frac{3}{4\pi\sigma_j^3}\int_{|\boldsymbol{r_2}-\boldsymbol{r_1}|<\sigma_j} d\boldsymbol{r_2}\rho_j(\boldsymbol{r_2}). \quad (18)$$

The derivative of the free energy contribution association with respect to segment density when the different segments in the system are of different sizes can be written as

$$\frac{\delta\beta A^{ex,assoc}}{\delta\rho_i(\boldsymbol{r})} = \sum_{A\in\Gamma^i}(\ln\chi_A^i(\boldsymbol{r})) - \frac{1}{2}\iint d\boldsymbol{r_1}d\boldsymbol{r_2}\sum_{j=1}^{N}\sum_{k=1}^{N}\rho_j(\boldsymbol{r_1})\rho_k(\boldsymbol{r_2}) \times \sum_{A\in\Gamma^j}\sum_{B\in\Gamma^k}\chi_A^j(\boldsymbol{r_1})\chi_B^k(\boldsymbol{r_2})\left(\frac{\delta\ln y^{jk}(\boldsymbol{r_1},\boldsymbol{r_2})}{\delta\rho_i(\boldsymbol{r})}\right). \quad (19)$$

The chain contribution can be obtained from the association free energy by letting the association energy go to infinity ($\varepsilon_{Ai,Bk}^{assoc}\to\infty$) and having an additional bond energy $\upsilon_{bond}^{ik}(\boldsymbol{r_1},\boldsymbol{r_2})$ for tangentially bonded segments. Taking the derivative of the chain term and inserting into Eq. (9) gives[39]

$$\ln\rho_i(\boldsymbol{r}) + \sum_{A\in\Gamma^i}\ln\chi_A^k(\boldsymbol{r}) - \frac{1}{2}\sum_{j=1}^{N}\sum_{k}^{\{k\}}\int\rho_j(\boldsymbol{r_1})\frac{\delta\ln y^{jk}[\{\bar{\rho}_m(\boldsymbol{r_1})\}]}{\delta\rho_i(\boldsymbol{r})}d\boldsymbol{r_1} + \frac{\delta\beta A^{ex,HS}}{\delta\rho_i(\boldsymbol{r})} + \frac{\delta\beta A^{ex,att}}{\delta\rho_i(\boldsymbol{r})} + \frac{\delta\beta A^{ex,assoc}}{\delta\rho_i(\boldsymbol{r})} = \beta(\mu^{bulk} - V_{ext}(\boldsymbol{r})) \quad \text{for i} = 1\ldots\text{N}. \quad (20)$$

The summation in the second term on the left hand side is over all the chain forming sites. {k} is the set of all segments bonded to segment j. We can solve this equation iteratively to obtain the equilibrium density profile. Once the equilibrium density profile is known it can be used to calculate the properties of the system. The surface tension γ is calculated as

$$\gamma = \frac{\Omega - \Omega_{bulk}}{A}, \quad (21)$$

where Ω is the grand potential of the system, Ω_{bulk} is the bulk grand potential, and A is the surface area.

The bonding state of the molecule varying with distance from the surface is another property of interest in this system. Since the theory considers the different sites to be independent of each other the fraction of molecules having different number of bonds can be directly calculated from the fraction of molecules not bonded at a site. The fraction of alcohol molecules that are monomers (X_0), bonded at one site (X_1), and bonded at both the sites (X_2) is given by

$$X_0 = \left(\chi_A^{alcohol}\right)^2, \quad (22a)$$

$$X_1 = 2\left(\chi_A^{alcohol}\right)\left(1-\chi_A^{alcohol}\right), \quad (22b)$$

$$X_2 = \left(1-\chi_A^{alcohol}\right)^2. \quad (22c)$$

The fraction of water molecules is not bonded at all (X_0), bonded at one site (X_1), bonded at two sites (X_2), bonded at three sites (X_3), and bonded at all four sites (X_4) can be similarly obtained and is given in Ref. 46.

TABLE I. Pure component parameter: Chain length (m), segment diameter (σ), long-range attraction energy for the hydrophilic segment (ε_{att}/k), association energy for association (ε_{assoc}/k), and bond volume (κ).

	m	σ (Å)	ε_{att}/k (K)	ε_{assoc}/k (K)	κ
Water	1	2.98	305.1	1850	0.0584
Methanol	1	3.61	303.5	3060	0.02183
Ethanol	2	3.17	305.2	3028	0.02512
1-Propanol	3	3.1	440	2655	0.01689
2-Propanol	3	3.1	420	2334	0.02512

C. Parameters

The parameters for the inhomogeneous system are obtained from bulk phase properties, so the inhomogeneous properties calculated are purely predictive. There are four pure component parameters: segment diameter (σ), long-range attraction energy (ε_{att}), association energy ε_{assoc}, and bond volume (κ) (Table I). Since the alcohol has hydrophilic (segments with hydrogen bonding sites) and hydrophobic segments, the long-range attraction energy for the segments would be different due to the presence of polar interactions between hydrophilic segments. We assume that ε_{att} for the hydrophobic segment of an alcohol is the same as the long range attraction energy of the corresponding alkane; for example, $\varepsilon_{att}^{hydrophobic}$ for ethanol is obtained from ethane. $\varepsilon_{att}^{hydrophobic} = 225.5$ and 219 for ethanol and propanol, respectively. Methanol is modeled as a single sphere and does not have separate hydrophobic and hydrophilic segments. It is not a great model for methanol, but having two different segments would mean having a very small segment size. Since the interest here is to study the trends in alcohols methanol is modeled with one sphere, ethanol with two spheres, and propanol with three spheres. $\varepsilon_{att}^{hydrophilic}$ along with σ, ε_{assoc}, and κ are fit to saturated liquid density and vapor pressure. The binary interaction parameter k_{AW} for the different water-alcohol mixtures (Table II) is obtained by adjusting to the binary phase diagrams (shown in Figure 2). Water and alcohol molecules interact with the hydrophobic surface through an external hard wall potential.

III. RESULTS AND DISCUSSION

This section describes the structure and thermodynamic properties of water-alcohol mixtures at a hydrophobic surface. Figure 3 shows the interfacial tension for aqueous mixtures of methanol, ethanol, 1-propanol, and 2-propanol with varying alcohol concentration at 293 K and 1 atm. Since there is no experimental interfacial tension data at a liquid-solid interface for water-alcohol mixtures, we compare against interfacial tension for a liquid-vapor interface.[57] Pratt and Chandler made the observation that since water dewets a hydrophobic surface, it is as if a vapor layer is present between the liquid and the surface. So water at a hydrophobic surface is similar to water at a liquid-vapor interface.[58,59] This should be valid for aqueous alcohol mixtures as well since both water and alcohol dewet the surface. The agreement of the theoretical prediction with the experimental data is very good.

Interfacial tension of pure water is very high compared to alcohols and the addition of a small amount of alcohol decreases its interfacial tension drastically. A decrease in interfacial tension is also seen by a decrease in the contact angle of a water droplet at a hydrophobic surface with the addition of alcohol.[27] The interfacial tension of the alcohol mixtures is different at a given alcohol concentration with aqueous methanol having the highest interfacial tension and aqueous propanol having the lowest interfacial tension. An interesting observation is that at low concentrations, the 1-propanol mixture has a lower interfacial tension than the 2-propanol mixture.

TABLE II. Binary parameter k_{AW} for water-alcohol mixture.

	k_{AW}
Methanol	– 0.065
Ethanol	– 0.042
1-Propanol	– 0.03
2-Propanol	– 0.054

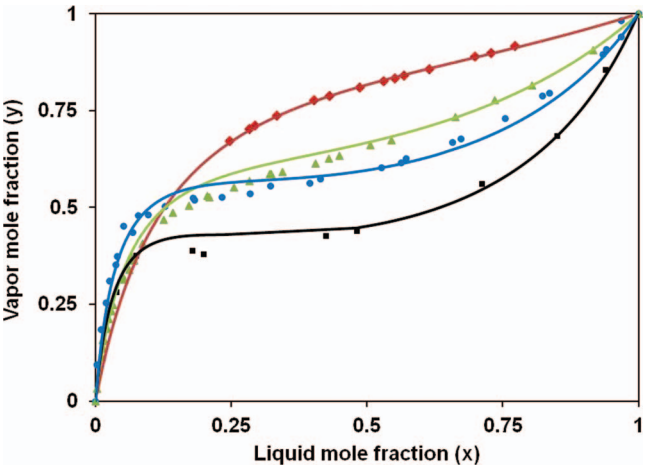

FIG. 2. x-y phase diagram for water-alcohol systems. Symbols are experimental data[62–64] and lines are obtained from theory. Methanol (red), ethanol (green), 1-propanol (black), and 2-propanol (blue).

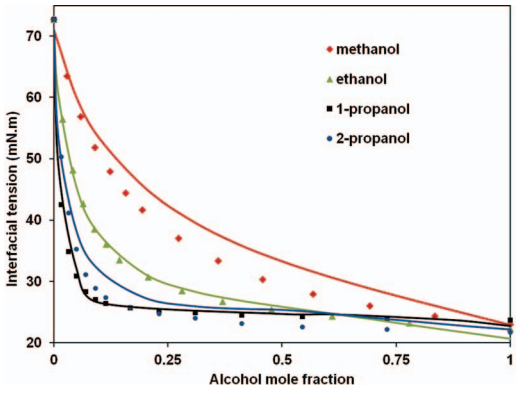

FIG. 3. Surface tension of alcohol with varying alcohol mole fraction for methanol (red), ethanol (green), 1-propanol (black), and 2-propanol (blue). Symbols are experimental data[57] and lines are theoretical predictions.

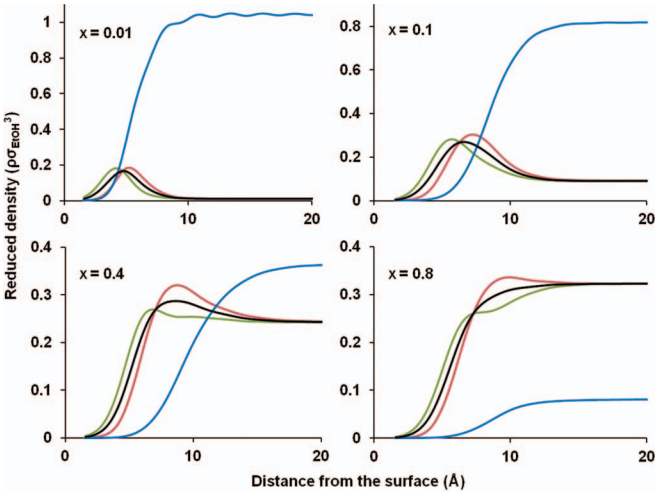

FIG. 4. Structure of ethanol-water mixture next to a hydrophobic surface with varying ethanol concentration. The hydrophobic surface is on the left and bulk liquid on the right. Water density (blue), average ethanol density (black), hydrophobic ethanol segment (green), and hydrophilic ethanol segment (red).

The decrease in interfacial tension can be explained by looking at the molecular structure of water and alcohol next to the surface. The hydrophobic surface interferes with the hydrogen-bonded network of water so it dislikes being next to the surface and has a high interfacial tension. Addition of alcohol, which has both hydrophobic and hydrophilic segments, stabilizes the structure with the hydrophobic segment of alcohol preferentially going to the hydrophobic surface and the hydrophilic segment facing away from the surface and towards bulk water. Molecular simulation studies of a water-ethanol mixture at a PDMS surface also show orientation ordering of ethanol with the hydrophobic segment of ethanol facing the surface and hydrophilic segment facing away from the surface.[17] Figure 4 shows the structure of water and ethanol at different mole fractions of ethanol. With increasing ethanol concentration, ethanol density close to the surface increases and the maximum in its average density moves away from the surface. As ethanol concentration increases, more water molecules get displaced from near the surface but the number of molecules getting displaced does not increase linearly with bulk ethanol concentration. At low concentrations, a large number of water molecules are displaced but as more and more ethanol molecules are added into the system, the surface becomes saturated and further addition of ethanol does not change the surface concentration much. This effect can be seen in the interfacial tension curve as well with a steep decrease in interfacial tension at low alcohol concentrations, but not much decrease at higher concentrations. The presence of the surface affects the properties of the system at lower concentrations of alcohol until the surface is saturated with alcohol. Once it is saturated, there is little effect of the surface on the properties of the system.

Figure 5 shows the reduced density profile of water with methanol, ethanol, 1-propanol, and 2-propanol at an alcohol bulk mole fraction of 0.05. As we go from methanol to propanol, the size of the hydrophobic group increases while the size of the hydrophilic group remains the same. With the alcohols orienting themselves perpendicular to the surface, propanol is most effective in keeping the water far from the surface preserving its structure. We can draw parallels between alcohols and surfactants which are structurally similar to alcohols having hydrophobic and hydrophilic groups bonded to each other. For surfactants, increasing the size of the hydrophobic tail length (equivalent to going from

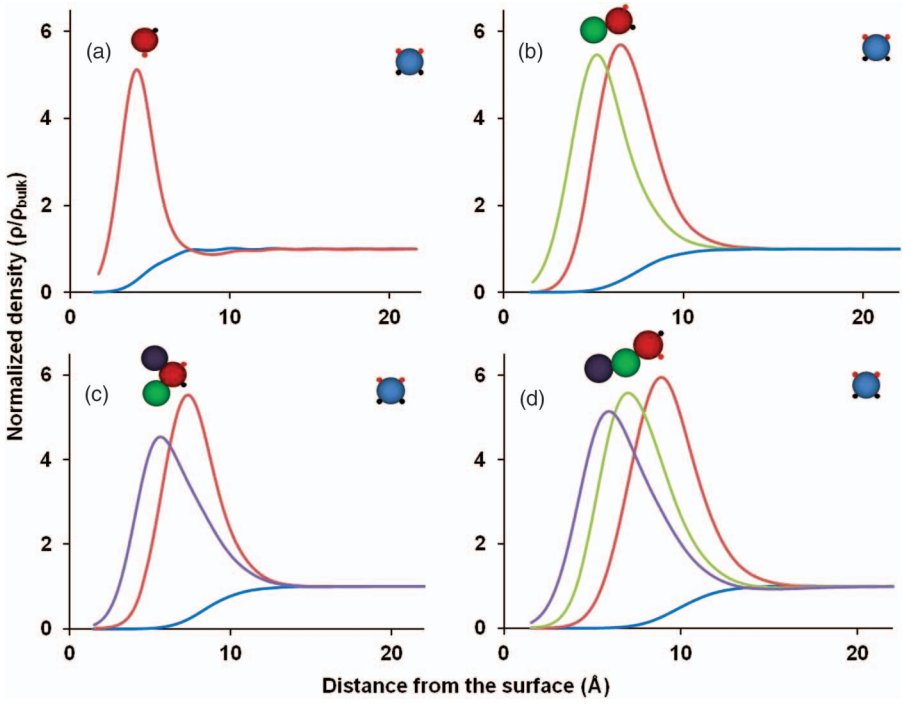

FIG. 5. Density profile for water-alcohol mixtures at a hydrophobic surface normalized to its bulk density at $x_{alcohol} = 0.05$. (a) Methanol, (b) ethanol, (c) 2-propanol, and (d) 1-propanol. The different curves represent the different segments on the chain as shown by the schematics.

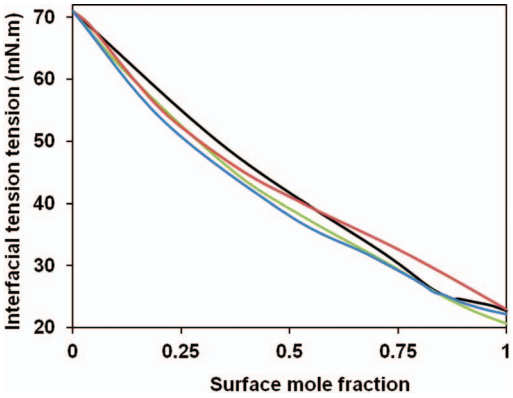

FIG. 6. Interfacial tension varying with surface mole fraction. Color scheme is the same as Figure 3.

methanol to propanol) increases the effectiveness of surfactant in reducing the interfacial tension.[60] Comparison of the structure of 1- and 2-propanol is interesting because they both have the same size of hydrophobic group but in 1-propanol the hydrophilic segment is an end segment while in 2-propanol it is a middle segment. At low concentrations, the two hydrophobic segments of 1-propanol can pack the surface well keeping the hydrogen bonding network far from the surface. 2-propanol on the other hand has both end hydrophobic segments next to the surface (as shown by the schematic in Figure 5) and there is stronger excluded volume effects causing fewer 2-propanol molecules to go to the surface. So the concentration of 2-propanol at the surface is lower than that of 1-propanol despite having the same concentration in the bulk. The fact that 1-propanol has a lower interfacial tension is not surprising if we compare it to surfactants. It is known that a higher bulk concentration of two tail surfactants (which has a structure like 2-propanol) is required to achieve the same interfacial tension as a one tail surfactant (which has a structure like 1-propanol).[60,61]

Another way to look at how structuring affects the properties is to see the interfacial tension varying with surface mole fraction. We define the surface mole fraction of the alcohols as the average mole fraction of the alcohol in the first three alcohol molecular layers next to the hydrophobic surface (~10 Å). The surface mole fraction is sensitive to the region defined as the surface region and increasing the surface region decreases the surface mole fraction. Figure 6 shows interfacial tension curves for the different alcohols almost overlap with one another implying that for a given mole fraction of alcohol, the different alcohol mixtures have similar values of interfacial tension. It is important to recognize that this trend is not true for interfacial tension varying with the number of alcohol molecules at the surface (surface loading) but with the mole fraction of alcohols at the surface. Increasing the mole fraction of alcohol not only means an increase in the number of alcohol molecules but also a decrease in water molecules. So it is important to know how the alcohol molecules partition to the surface and how effective they are in keeping water molecules away from the surface.

The effectiveness of the alcohols in displacing water molecules next to the hydrophobic surface and reducing unfavorable interactions of water with the surface can be seen in Figure 7. The figure on the left (Figure 7(a)) is the average alcohol density reduced by the average bulk density of the alcohol at an alcohol mole fraction of 0.05. Since the size of a methanol molecule is small, its average density is very high close to the surface. As the size of the alcohol chain molecule increases, the maximum in its average density moves away from the surface. The number of molecules going to the surface also decreases since the number of configurations these chain molecules can take decreases next to the surface and there is a larger penalty to be next to the surface. Since 2-propanol has both end hydrophobic segments pointing towards the surface its maximum in average density is closer to the surface than 1-propanol. The figure on the right shows the water density profiles reduced by bulk water density with these different alcohols (Figure 7(b)). For water, when there is no alcohol, its density profile is close to the surface (gray dotted curve); addition of alcohol pushes the density profile away from the surface. Even though the number density of propanol is lower than methanol, the volume occupied by the propanol molecules is higher and so it is more effective in displacing the water away from the surface. Even though methanol has the highest number density close to the surface, it still has a low surface concentration.

Surface concentration is an important quantity for separation processes since the interest there is in the alcohol preferentially going to the surface. Figure 8 shows the surface mole

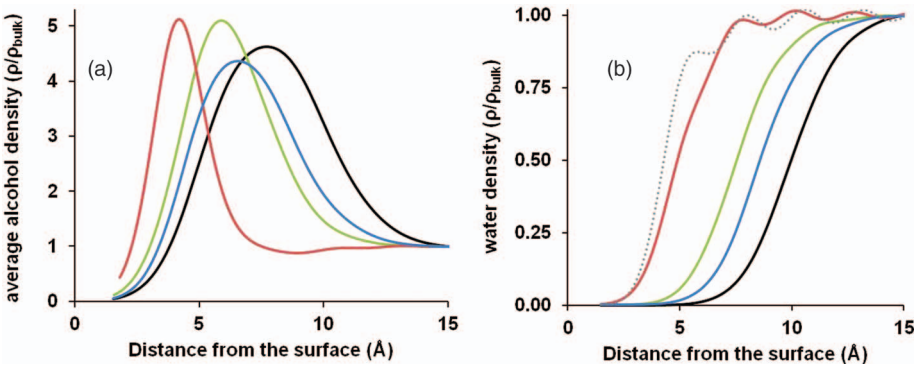

FIG. 7. Normalized average alcohol (left) and water density (right) ($\frac{\rho}{\rho_{bulk}}$) for the different alcohols at an alcohol mole fraction x = 0.05; methanol (red), ethanol (green), 2-propanol (blue), and 1-propanol (black). The gray dotted curve in (b) is the normalized density for pure water (with no alcohol).

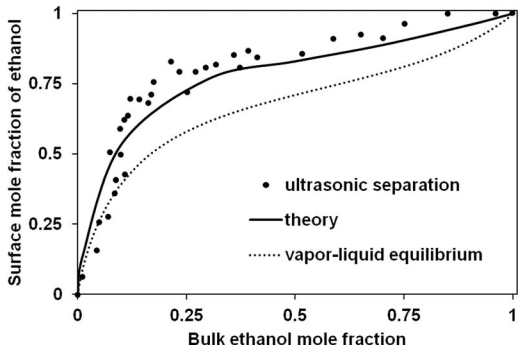

FIG. 8. Surface mole fraction of ethanol versus bulk ethanol mole fraction. The solid curve is the theoretical prediction, dotted curve is the vapor-liquid equilibrium curve, and the symbols are mole fraction in the mist obtained from ultrasonic separation.

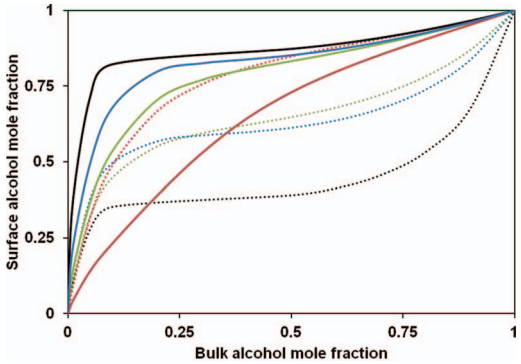

FIG. 9. Surface mole fraction of alcohol. Methanol (red), ethanol (green), 1-propanol (black), and 2-propanol (blue). Solid curves are surface mole fraction and dotted curves are vapor-liquid equilibrium.

fraction versus the bulk mole fraction of ethanol as predicted by theory (solid line) at 303 K. The surface mole fraction of ethanol is high even for low bulk mole fractions showing a preferential adsorption of ethanol at the surface. The dotted line is the vapor mole fraction versus the liquid mole fraction (x-y diagram) for a vapor-liquid equilibrium system. A higher surface mole fraction of ethanol compared to its mole fraction in the vapor indicates that a technique to harvest the surface layer could provide a larger separation of ethanol as compared to what is obtained in the vapor. The dots are experimental results for the mole fraction of ethanol in the mist (obtained from a liquid-vapor interface by ultrasonic separation) versus its bulk mole fraction in the liquid.[15] Since the mist is comprised of droplets obtained from the vapor-liquid interface, it is similar to a surface mole fraction at a vapor-liquid interface and compares well with the surface mole fraction calculated theoretically here. At low alcohol concentrations, the ultrasonic separation follows the vapor liquid equilibrium curve but at higher alcohol concentrations it follows the curve for surface concentration at a hydrophobic surface. It is interesting to note that this switch occurs at around the same concentration where the interfacial tension curve flattens out. It might point towards the fact that at higher concentrations of alcohol, the mist droplets have enough alcohol to stabilize the droplet and hence it resembles the concentration curve of a water-alcohol mixture at a hydrophobic surface. The correlation between droplet size, concentration of alcohol required to stabilize the droplet, and the interfacial tension is something that needs to be studied further.

Figure 9 compares the surface mole fraction (solid curves) of the different alcohols with their vapor-liquid coexistence curves (dotted curves) at 293 K. As the chain length increases, the vapor pressure of the molecule decreases and it becomes harder for the molecule to go into the vapor phase. And so the y-x curve shifts downwards as we go from methanol to propanol. But the surface mole fraction has the opposite trend with the surface mole fraction increasing from methanol to propanol. So for methanol, the vapor mole fraction is higher than the surface mole fraction but the advantage of using the surface over liquid-vapor interface for separation

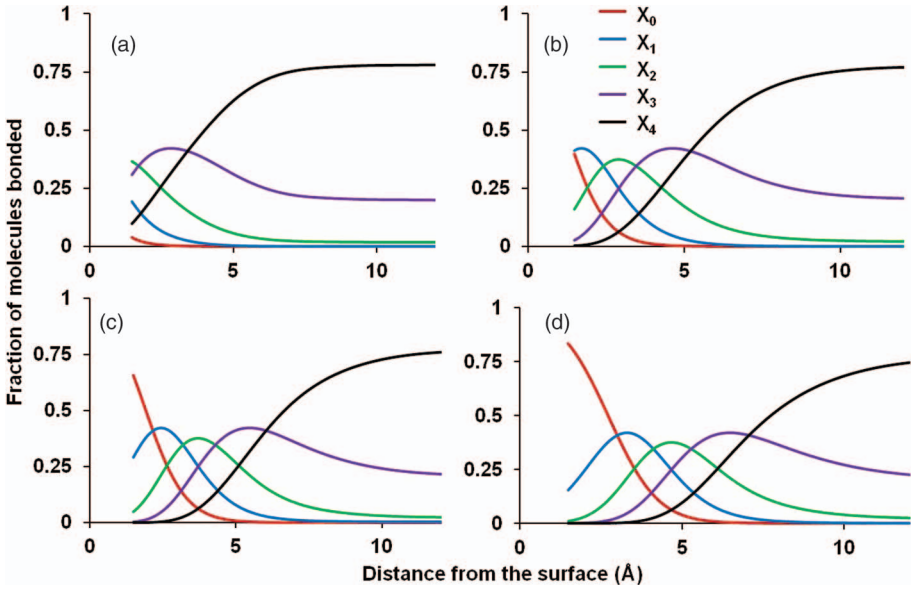

FIG. 10. Hydrogen bonding in water at an alcohol mole fraction of 0.05. Fraction of water molecules not bonded at all (X_0), bonded at one site (X_1), bonded at two sites (X_2), bonded at three sites (X_3), and bonded at four sites (X_4). Water in a mixture with (a) methanol, (b) ethanol, (c) 2-propanol, and (d) 1-propanol.

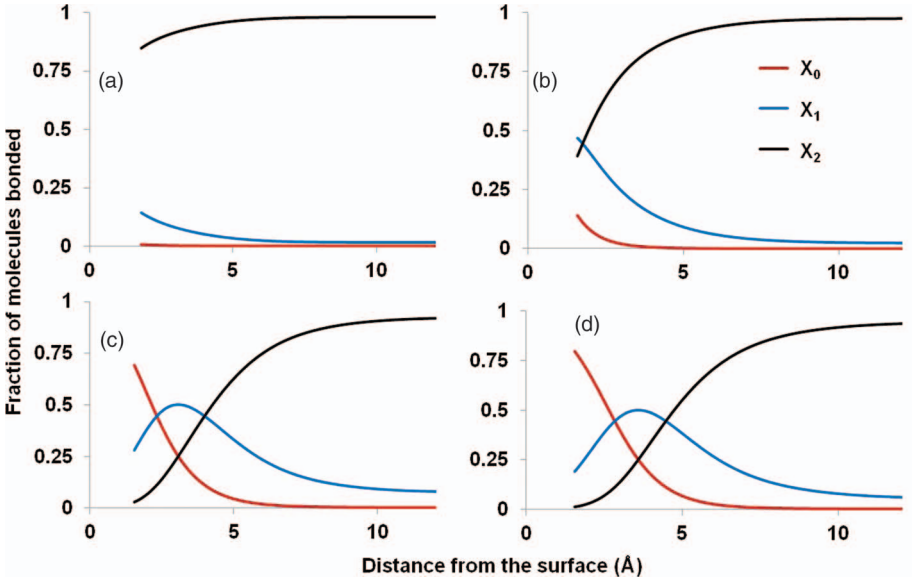

FIG. 11. Hydrogen bonding in alcohol at an alcohol mole fraction of 0.05. Fraction of alcohol molecules not bonded at all (X_0), bonded at one site (X_1), and bonded at both sites (X_2). (a) Methanol, (b) ethanol, (c) 2-propanol, and (d) 1-propanol.

becomes apparent for ethanol and propanol with the highest difference being for 1-propanol.

An important feature of the water-alcohol systems is its hydrogen bonding structure. Figure 10 shows the fraction of water molecules in the mixture that are not bonded at all (X_0), bonded at one site (X_1), bonded at two sites (X_2), bonded at three sites (X_3), and bonded at all four sites (X_4) at an alcohol mole fraction of 0.05. The fraction includes water molecules bonded to other water molecules and to alcohol molecules. Since water can form up to four hydrogen bonds, its bonding network is severely affected by the presence of a hydrophobic surface. Far away from the surface, 75% of the water molecules are bonded at all four sites whereas close to the surface the fraction of molecules that are bonded at all four sites is close to zero. Water thus pays a huge entropic penalty to be next to the surface. The success of alcohol in preserving the hydrogen-bonded network of water depends on the structure of the molecules in the mixture. Most water molecules in the mixture with methanol are at least bonded at one site since both water and methanol segments are present close to the surface (Figure 10(a)). This is in strong contrast to the water in a mixture with 1-propanol where about 83% of water molecules in contact with the surface are not bonded at all (Figure 10(d)). Since the two hydrophobic segments of 1-propanol go towards the surface and displace most of the water molecules, a water molecule present next to the surface is unable to form any hydrogen bonds. Comparing 1-propanol and 2-propanol, the peaks in X_1, X_2, and X_3 occur closer to the surface in 2-propanol than in 1-propanol since the water molecules and the hydrophilic segments of 2-propanol are present closer to the surface. Figure 11 shows the fraction of alcohol molecules that are monomers (X_0), bonded at one site (X_1) and bonded at both sites (X_2). For methanol, most of the molecules next to the surface are bonded at both sites. Even for ethanol, most hydrophilic segments are bonded either at one (X_1) or both sites (X_2). But for 1- and 2-propanol, a large fraction of hydrophilic segments next to the surface are not bonded at all since that region contains mainly hydrophobic segments. It should be noted that though the fraction of alcohol monomers close to the surface is large, the density of the hydrophilic segment of the alcohol is very small in that region and so the density of monomers would be small.

The next step would be to look at mixtures of multiple alcohols in aqueous solution. An example is shown in Figure 12 which shows the structuring of an aqueous mixture of 1- and 2-propanol ($x_{1\text{-propanol}} = x_{2\text{-propanol}} = 0.05$). Density of 1-propanol (solid curve) is higher than 2-propanol (dotted curve) close to the surface again showing better partitioning of 1-propanol to the surface. 1-propanol also spreads out more next to the surface as compared to 2-propanol (the density profile for the two hydrophobic segments of 2-propanol lie on top of each other because of the symmetry in the molecule). The value of interfacial tension of this mixture is between the

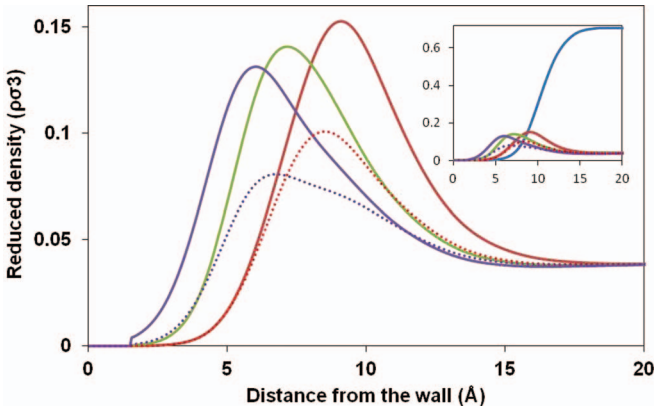

FIG. 12. Structure of aqueous mixture of 1- and 2-propanol where the mole fraction of both 1- and 2-propanol is 0.05 each. The solid lines are 1-propanol density and the dotted lines are 2-propanol density. The color scheme is the same as Figure 5. The inset shows the same mixture zoomed out to show the water profile.

interfacial tension of water-1-propanol and water-2-propanol at the same alcohol concentration.

IV. CONCLUSIONS

We have studied the molecular structure and interfacial properties of aqueous mixtures of short alcohols at a hydrophobic surface with varying alcohol concentration using interfacial iSAFT. The drastic reduction of the interfacial tension of water at the surface with the addition of alcohol can be understood by looking at the structuring of water and alcohol near the surface. The presence of a hydrophobic surface disrupts the hydrogen-bonded network of water so it pays a large entropic penalty to be next to the surface. The alcohols, containing both hydrophobic and hydrophilic segments, preferentially go to the surface with the hydrophobic segments facing towards the surface and the hydrophilic segments facing bulk water. The different alcohols with different relative sizes of the hydrophobic and hydrophilic groups, structure next to the surface in different ways and thus reduce interfacial tension to different degrees. For the same bulk concentration of alcohol, the interfacial tension decreases with increasing hydrophobic group size of the alcohol (from methanol to propanol). Since 2-propanol has a larger excluded volume it does not partition to the surface well and at low bulk concentrations it has a higher interfacial tension than 1-propanol. Interfacial tension has a strong dependence on surface mole fraction with all the alcohols giving similar values of interfacial tension for a given surface mole fraction. This information is important for separation of water-alcohol mixtures at liquid-solid interfaces. With the exception of methanol, mole fraction of alcohols is found to be higher at the surface than that obtained in the vapor in equilibrium with a liquid making it a better system for separation of alcohol from water. The obtained structure is also important to understand the mechanism involved in ultrasonic separation.

ACKNOWLEDGMENTS

We gratefully acknowledge the financial support of Robert A Welch Foundation (Grant No. 1241).

[1]S. Y. Noskov, M. Kiselev, and A. Kolker, J. Struct. Chem. **40**(2), 253–261 (1999).
[2]G. C. Benson and O. Kiyohara, J. Solution Chem. **9**(10), 791–804 (1980).
[3]F. Franks and D. J. G. Ives, Q. Rev. Chem. Soc. **20**(1), 1–44 (1966).
[4]E. J. Wensink, A. C. Hoffmann, P. J. van Maaren, and D. van der Spoel, J. Chem. Phys. **119**, 7308 (2003).
[5]T. Sato, A. Chiba, and R. Nozaki, J. Chem. Phys. **112**, 2924 (2000).
[6]T. Sato, A. Chiba, and R. Nozaki, J. Chem. Phys. **113**, 9748 (2000).
[7]S. Dixit, A. Soper, J. Finney, and J. Crain, Europhys. Lett. **59**(3), 377 (2002).
[8]J. L. Finney, D. T. Bowron, R. M. Daniel, P. A. Timmins, and M. A. Roberts, Biophys. Chem. **105**(2–3), 391–409 (2003).
[9]T. S. van Erp and E. J. Meijer, J. Chem. Phys. **118**, 8831 (2003).
[10]J. Fidler and P. Rodger, J. Phys. Chem. B **103**(36), 7695–7703 (1999).
[11]S. Dixit, J. Crain, W. C. K. Poon, J. L. Finney, and A. K. Soper, Nature (London) **416**(6883), 829–832 (2002).
[12]D. González-Salgado and I. Nezbeda, Fluid Phase Equilib. **240**(2), 161–166 (2006).
[13]P. Petong, R. Pottel, and U. Kaatze, J. Phys. Chem. A **104**(32), 7420–7428 (2000).
[14]J. G. Davis, K. P. Gierszal, P. Wang, and D. Ben-Amotz, Nature (London) **491**(7425), 582–585 (2012).
[15]M. Sato, K. Matsuura, and T. Fujii, J. Chem. Phys. **114**, 2382 (2001).
[16]J. Weitkamp, S. Ernst, B. Günzel, and W.-D. Deckwer, Zeolites **11**(4), 314–317 (1991).
[17]L. Fritz and D. Hofmann, Polymer **38**(5), 1035–1045 (1997).
[18]G. Onori and A. Santucci, J. Mol. Liq. **69**, 161–181 (1996).
[19]J. F. Brandts and L. Hunt, J. Am. Chem. Soc. **89**(19), 4826–4838 (1967).
[20]Y. Nozaki and C. Tanford, J. Biol. Chem. **246**(7), 2211–2217 (1971).
[21]K. Gekko and S. N. Timasheff, Biochemistry **20**(16), 4667–4676 (1981).
[22]M. Matsumoto, Y. Takaoka, and Y. Kataoka, J. Chem. Phys. **98**, 1464 (1993).
[23]T.-M. Chang and L. X. Dang, J. Phys. Chem. B **109**(12), 5759–5765 (2005).
[24]Y. Kanda, T. Nakamura, and K. Higashitani, Colloids Surf., A **139**(1), 55–62 (1998).
[25]H. Shinto, M. Miyahara, and K. Higashitani, Langmuir **16**(7), 3361–3371 (2000).
[26]M. Ø. Jensen, O. G. Mouritsen, and G. H. Peters, J. Chem. Phys. **120**, 9729 (2004).
[27]T. Soeno, K. Inokuchi, and S. Shiratori, Appl. Surf. Sci. **237**(1–4), 539–543 (2004).
[28]L. Zhai, M. C. Berg, F. Ç. Cebeci, Y. Kim, J. M. Milwid, M. F. Rubner, and R. E. Cohen, Nano Lett. **6**(6), 1213–1217 (2006).
[29]M. Lundgren, N. L. Allan, T. Cosgrove, and N. George, Langmuir **18**(26), 10462–10466 (2002).
[30]M. Yaacobi and A. Ben-Naim, J. Solution Chem. **2**(5), 425–443 (1973).
[31]W. G. Chapman, Ph.D. thesis, Cornell University, 1988.
[32]M. S. Wertheim, J. Stat. Phys. **42**(3), 459 (1986).
[33]E. Kierlik and M. L. Rosinberg, J. Chem. Phys. **97**(12), 9222–9239 (1992).
[34]E. Kierlik and M. L. Rosinberg, J. Chem. Phys. **99**(5), 3950–3965 (1993).
[35]C. J. Segura, W. G. Chapman, and K. P. Shukla, Mol. Phys. **90**, 759 (1997).
[36]Y.-X. Yu and J. Wu, J. Chem. Phys. **116**(16), 7094–7103 (2002).
[37]Y.-X. Yu and J. Wu, J. Chem. Phys. **117**(5), 2368–2376 (2002).
[38]S. Tripathi and W. G. Chapman, J. Chem. Phys. **122**(9), 094506 (2005).
[39]S. Jain, A. Dominik, and W. G. Chapman, J. Chem. Phys. **127**(24), 244904–244912 (2007).
[40]W. G. Chapman, K. E. Gubbins, G. Jackson, and M. Radosz, Fluid Phase Equilib. **52**, 31–38 (1989).
[41]A. Dominik, S. Tripathi, and W. G. Chapman, Ind. Eng. Chem. Res. **45**(20), 6785–6792 (2006).
[42]S. Jain and W. G. Chapman, Mol. Phys. **107**(1), 1–17 (2009).
[43]C. P. Emborsky, Z. Feng, K. R. Cox, and W. G. Chapman, Fluid Phase Equilib. **306**(1), 15–30 (2011).
[44]A. Bymaster and W. G. Chapman, J. Phys. Chem. B **114**(38), 12298–12307 (2010).
[45]Z. Feng, A. Bymaster, C. Emborsky, D. Ballal, B. Marshall, K. Gong, A. Garcia, K. R. Cox, and W. G. Chapman, J. Stat. Phys. **145**(2), 467–480 (2011).
[46]A. Bymaster, A. Dominik, and W. G. Chapman, J. Phys. Chem. C **111**(43), 15823–15831 (2007).
[47]B. D. Marshall, K. R. Cox, and W. G. Chapman, J. Phys. Chem. C **116**(33), 17641–17649 (2012).
[48]H. Kahl and S. Enders, Fluid Phase Equilib. **172**(1), 27–42 (2000).
[49]Z.-Y. Zhang, J.-C. Yang, and Y.-G. Li, Fluid Phase Equilib. **169**(1), 1–18 (2000).
[50]I. Nezbeda, J. Pavlíček, J. Kolafa, A. Galindo, and G. Jackson, Fluid Phase Equilib. **158–160**, 193–199 (1999).
[51]J. D. Weeks, D. Chandler, and H. C. Andersen, J. Chem. Phys. **54**(12), 5237–5247 (1971).
[52]W. Bol, Mol. Phys. **45**, 605–616 (1982).
[53]W. G. Chapman, G. Jackson, and K. E. Gubbins, Mol. Phys. **65**, 1057–1079 (1988).
[54]Y. Rosenfeld, Phys. Rev. Lett. **63**, 980 (1989).
[55]T. Kraska and K. E. Gubbins, Ind. Eng. Chem. Res. **35**(12), 4727–4737 (1996).
[56]G. N. Clark, A. J. Haslam, A. Galindo, and G. Jackson, Mol. Phys. **104**(22–24), 3561–3581 (2006).
[57]G. Vazquez, E. Alvarez, and J. M. Navaza, J. Chem. Eng. Data **40**(3), 611–614 (1995).
[58]D. M. Huang and D. Chandler, J. Phys. Chem. B **106**(8), 2047–2053 (2002).

[59]T. R. Jensen, M. Ø. Jensen, N. Reitzel, K. Balashev, G. H. Peters, K. Kjaer, and T. Bjørnholm, Phys. Rev. Lett. **90**(8), 086101 (2003).
[60]C. P. Emborsky, K. R. Cox, and W. G. Chapman, J. Chem. Phys. **135**, 084708 (2011).
[61]L. Rekvig, M. Kranenburg, J. Vreede, B. Hafskjold, and B. Smit, Langmuir **19**(20), 8195–8205 (2003).
[62]K. Kurihara, T. Minoura, K. Takeda, and K. Kojima, J, Chem. Eng. Data **40**(3), 679–684 (1995).
[63]R. M. Rieder and A. R. Thompson, Ind. Eng. Chem. **41**(12), 2905–2908 (1949).
[64]P. Murti and M. Van Winkle, Ind. Eng. Chem. Chem. Eng. Data Ser. **3**(1), 72–81 (1958).